VI International Conference on Computational Methods in Marine Engineering
MARINE 2015
F. Salvatore, R. Broglia and R. Muscari (Eds)

CFD, POTENTIAL FLOW AND SYSTEM-BASED SIMULATIONS OF FULLY APPENDED FREE RUNNING 5415M IN CALM WATER AND WAVES

Hamid Sadat-Hosseini[*], Serge Toxopeus[†], Michel Visonneau[‡], Emmanuel Guilmineau[‡], Tin-Guen Yen[♠], Woei-Min Lin[♣], Gregory Grigoropoulos[♯] and Frederick Stern[*]

[*] IIHR - Hydroscience & Engineering, The University of Iowa

[†] Corresponding author
Maritime Research Institute Netherlands(MARIN)
Haagsteeg 2, 6708 PM, Wageningen, The Netherlands
Email: s.l.toxopeus@marin.nl Web page: http://www.marin.nl

[‡] ECN - Ecole Centrale de Nantes

[♠] Leidos

[♣] Formerly SAIC, Currently ONRG

[♯] National Technical University of Athens

Key words: 5415M, course-keeping, waves, CFD, validation, NATO AVT-161

Abstract. *The seakeeping ability of ships is one of the aspects that needs to be assessed during the design phase of ships. Traditionally, potential flow calculations and model tests are employed to investigate whether the ship performs according to specified criteria. With the increase of computational power nowadays, advanced computational tools such as Computational Fluid Dynamics (CFD) become within reach of application during the assessment of ship designs. In the present paper, a detailed validation study of several computational methods for ship dynamics is presented. These methods range from low-fidelity system-based methods, to potential flow methods, to high-fidelity CFD tools. The ability of the methods to predict motions in calm water as well as in waves is investigated. In calm water, the roll decay behavior of a fully appended self-propelled free running 5415M model is investigated first. Subsequently, forced roll motions simulated by oscillating the rudders or stabilizer fins are studied. Lastly, the paper discusses comparisons between experiments and simulations in waves with varying levels of complexity, i.e. regular head waves, regular beam waves and bi-chromatic waves.*

The predictions for all methods are validated with an extensive experimental data set for ship motions and loads on appendages such as rudders, fins and bilge keels. Comparisons between the different methods and with the experiments are made for the relevant motions and the high fidelity CFD results are used to explain some of the complex physics. The course keeping and seakeeping of the model, the reduction rate of the roll motion, the effectiveness of the fin stabilizers as roll reduction device and the interaction of the roll motion with other motions are investigated as well. The paper shows that only high-fidelity CFD is able to accurately predict all the relevant physics during roll decay, forced oscillation and sailing in waves.

1 INTRODUCTION

The simulation of ship course keeping and seakeeping has mostly been studied using potential flow (PF) and system-based (SB) methods and more recently computational fluid dynamics (CFD). The assessment of the capability of these approaches is required to employ them in the ship design process. In the last two years, NATO AVT-161 and 216 groups under the NATO Science and Technology Organization were formed to assess the capability of the prediction methods for ship seakeeping and maneuvering in deep and shallow water. This paper is part of the work concentrating on the prediction capability in calm water, regular and bi-chromatic waves for deep water conditions which is conducted for 5415M surface combatant. The benchmark data for 5415M seakeeping were provided by MARIN. The data were collected for the 6DOF motions and forces and moments of the appendages such as bilge keels, rudders and stabilizer fins for different tests. The tests included roll decay and forced roll (by means of stabilizer fins or rudders) in calm water and seakeeping in regular, bi-chromatic and irregular waves. The measured data provided a unique opportunity to investigate the prediction capability of SB, PF and CFD methods for complicated 6DOF ship motions and forces and moments on the appendages.

In the past, SB models have been applied extensively to estimate ship maneuvering capabilities. The prediction capability of SB methods is strongly dependent on empirical formulae or the inputs for maneuvering coefficients, the degree of freedom of the model and the mathematical model techniques used to include the waves, the rudder and the propulsion forces. Therefore, SB predictions for different SB tools are different and they often show only qualitative results. Toxopeus and Lee [1] used several simulation tools to predict the maneuverability of different ship hulls including KVLCCs, 5415M and KCS. It was seen that the difference between SB predictions and the experiments depended strongly on the range of application of each prediction tool: MPP (originally made for full-block ships) provided good results for the KVLCCs, FreSim (for naval ships) for the 5415M and SurSim with slender body method (for cruise ships, ferries, motor yachts) for the KCS.

Unlike SB models, the PF methods employ strip theory, lifting line/surface or panel methods to compute directly the forces and moments used to predict 6DOF ship motions. However, empirical corrections to account for viscous effects are required (see Yen et al. [2] and Toxopeus and Lee [1]). An extensive benchmark study of state-of-the-art seakeeping prediction tools was presented by Bunnik et al. [3]. In this study, 11 different codes (9 PF codes and 2 CFD codes, of which one was ISIS-CFD) were used to calculate motions of ships in a seaway. Generally, it was found that good PF codes produce good results. When the motions are moderate and in the absence of large viscous effects, the benefit of using CFD instead of the best PF methods was found to be small.

In the last few years, CFD simulations have advanced from captive to free running 6DOF conditions with controllers and moving appendages and propellers, which provides the opportunity to study maneuvering, capsize and course keeping in calm water and waves. Maneuvering studies were presented first at SIMMAN 2008 for calm water condition (Stern et al. [4]). Sadat-Hosseini et al. [5][6] and Carrica et al. [7] presented maneuvering in calm water and regular waves for surface combatants (ONR tumblehome and 5415M) and surface effect ship (SES).

Table 1: DTMB5415M main particulars

Length : L	142.0 m	Natural period of roll	11.50 s
Breadth : B	19.06 m	Roll radii of gyration: k_{xx}	0.4*B
Draft : T	6.15 m	Pitch and yaw radius of gyration: k_{yy} k_{zz}	0.25L
Block coefficient : C_b	0.507	Propeller diameter: D_p	6.15 m
Transverse metacentric height: GM	1.95 m	Pitch at 0.7R: $P_{0.7R}$	5.32 m
Block coefficient : C_b	0.507	Expanded blade area ratio: A_E/A_0	0.58
Rudder area A_R	15.4m^2	Fin stabilizer area	6m^2

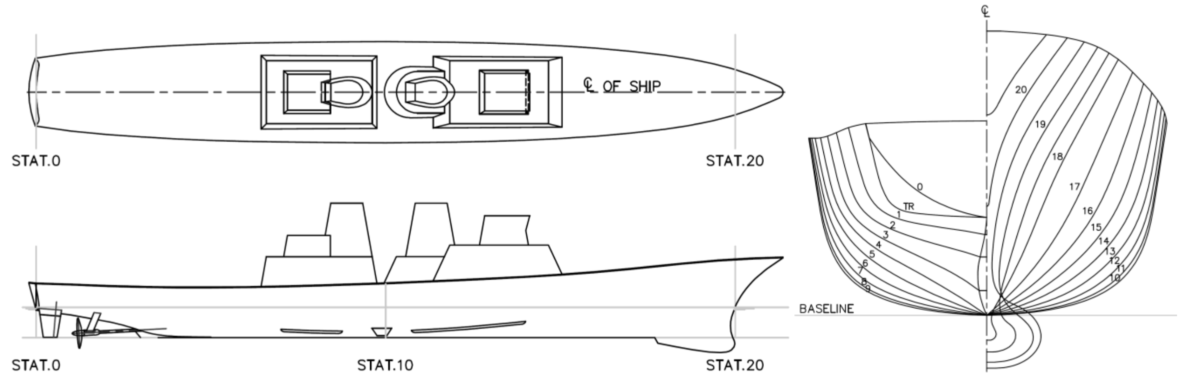

Figure 1: DTMB 5415M geometry and body plan

The most commonly used propeller model in the previous maneuvering studies is the axisymmetric body force method which is specified in a non-iterative manner such that the ship wake on the body force is neglected. Sadat-Hosseini et al. [8] studied propeller modeling effect on maneuvering using the fully discretized rotating propeller and two body force propeller models including non-iterative axisymmetric and interactive Yamasaki body force propeller models. Few research has focused on improving the SB mathematical model by using CFD with system identification (SI) methods for both calm water (Sadat-Hosseini et al. [5][8]; Araki et al. [9]) and following waves (Araki et al. [10]). The results were very promising in showing that the most accurate and efficient maneuvering coefficients can be obtained by CFD-based SI methods, which require few free running CFD simulations. Such an approach was also followed by Toxopeus [11] in which RANS calculations were used to derive coefficients for an SB model and the results of consecutive maneuvering simulations were compared with model experiments, demonstrating a large improvement compared to the simulations with the original coefficients derived from empirical formulae.

The objective of the present paper is to assess the capabilities of CFD, PF, and SB methods for course keeping in calm water and waves for 5415M as a benchmark test case for AVT-161. Herein, the results are investigated with consideration to the mathematical model of ship motions similar to the analysis performed for parametric rolling and broaching by Sadat-Hosseini et al. [5]. Also, a detailed validation study is performed for forces and moments on the appendages including rudders, fins and bilge keels and the high fidelity results are used to explain some of the complex physics.

Table 2: EFD, CFD, PF, and SB test cases in calm water and waves

Test Id.	Test Type	Fin Type	Selected Test Conditions	Codes
1.1	Free roll decay	Without Fin	ϕ_0=12 deg	SB: SurSim, FreSim PF: Fredyn, LAMP, SWAN2 CFD: CFDShip-Iowa, ISIS-CFD
1.2		Passive Fin	ϕ_0=-10 deg	SB: SurSim, FreSim PF: Fredyn, LAMP, SWAN2 CFD: CFDShip-Iowa, ISIS-CFD
1.3		Active Fin	ϕ_0=-18 deg	SB: SurSim, FreSim PF: Fredyn, LAMP CFD: CFDShip-Iowa
2.1	Forced roll due to rudders	Passive Fin	Amplitude=15 deg Period=11.42 s (full scale)	SB: SurSim, FreSim PF: Fredyn, LAMP CFD: CFDShip-Iowa
2.2		Active Fin	Amplitude=15 deg Period=11.42 s (full scale)	SB: SurSim, FreSim PF: Fredyn CFD: CFDShip-Iowa
2.3	Forced roll due to Fin	Forced Fin	Amplitude=25 deg Period=11.42 s (full scale)	SB: SurSim, FreSim PF: Fredyn, LAMP CFD: CFDShip-Iowa
3.1	Seakeeping in regular waves	Active Fin	H/λ=0.012,λ/L=1.205,μ=180 H/λ=0.0199,λ/L=0.678,μ=90	SB: SurSim, FreSim PF: Fredyn, LAMP CFD: CFDShip-Iowa
4.1	Seakeeping in bi-chromatic waves	Active Fin	H/ L: 0.035,λ/L: 0.97/1.14, μ:300deg	SB: SurSim, FreSim PF: Fredyn, LAMP CFD: CFDShip-Iowa

CFD computations are performed using the CFDShip-Iowa and ISIS-CFD codes. PF simulations are performed with Fredyn, SWAN and LAMP. The SB roll decay and forced roll predictions are carried out by using the SurSim and FreSim.

2 5415M TEST CASE

2.1 Hull form

Free running experiments in calm water and waves were conducted for 5415M. The 5415M model is a geosim of the DTMB 5415 ship model, but with modified appendages and skeg. Main particulars and body plan are shown in Table 1 and Figure 1, respectively. The model was manufactured of wood and appended with skeg, twin split bilge keels, roll stabilizer fins, twin rudders and rudder seats slanted outwards, shafts and struts, and counter-rotating propellers. The rudder was of the spade type. The lateral area of the rudders was $2\times15.4m^2$ i.e. 2×1.8% of the lateral area of the vessel, $L_{pp}\times T$. The propellers were fixed pitch type with direction of rotation inward over top. The stabilizer fins were of the non-retractable low aspect ratio type. The scale ratio of the model was 35.48.

2.2 Test Setup

All experiments were carried out in the MARIN Seakeeping and Maneuvering Basin. The tests were performed with the ship model free running and the propeller rate of revolutions adjusted to the self-propulsion point of the model for the envisaged speed. During the test, the wave elevation, ship motions, ship accelerations, rudder and fin angles and propellers revolutions were measured. Also, propeller torque and thrust and loads on bilge keels, rudders and fins were recorded. The wave elevations were measured in front of the vessel and beside the vessel at mid-ship using resistance-type wave probes and used to represent the wave elevation at center of gravity. The ship motions were recorded through optical tracking system. The ship accelerations were measured at three locations on the model using accelerometer. Several Potentio-meters were employed to measure rudder and fin angles. Strain gauge transducers were used to measure loads on the propellers, rudders, and fins. For loads on bilge keels, one-component force transducers were utilized. More details of the test setup can be found in Toxopeus et al. [12].

The coordinate system is ship-fixed located at centre of gravity, with x pointing toward the bow, y to portside and z upward. The roll (ϕ) is positive for starboard down, the pitch (θ) is positive for bow down and the yaw angle (ψ) is positive for bow turned to portside. The forces and moments are positive for X-force forwards, Y-force to portside, Z-force upward, K-moment pushing starboard into the water, M-moment pushing the bow into the water and N-moment pushing the bow to portside. The rudder angle (δ) is positive for trailing edge to portside and the stabilizer fin angles (δ_F) are positive for nose down position.

2.3 Test Conditions

A subset of the full experimental program with the self-propelled free model appended with passive, active, or no fin stabilizers was selected for the present study. The selection comprises roll decay and forced roll tests and tests in regular waves and in bi-chromatic waves. The conditions for different tests in calm water and waves are summarized in Table 2.

Herein, the cases are selected based on careful studies of the test results for validation of computations. All selected tests were conducted at a speed corresponding to Fn=0.248. In a roll decay test, the initial roll angle is applied by pushing the side of the model into the water. In forced roll, the roll motion is applied by moving the rudders or fins in a sinusoidal motion. The frequency of rudders or fins oscillation is 0.55Hz in full scale, which is close to the natural period of roll of the ship. For active fins cases, the fins are controlled with $\delta_F = D\dot{\varphi}$ autopilot controller in which D=5 sec in full scale. Also, the rudders are controlled by an autopilot controller, with $\delta = \delta_0 + P\psi + D\dot{\psi} + Ay$ but the controller settings were not recorded during the test. After the tests the coefficients δ_0, P, D and A were determined for each test individually by least-square fitting.

3 CFD METHOD

3.1 CFDShip-Iowa 4.5

CFDShip-Iowa is an overset, block structured CFD solver using non-orthogonal curvilinear coordinate system for arbitrary moving control volumes. Turbulence models include blended k-ε/k-ω based isotropic and anisotropic RANS and DES approaches. A single-phase level set method is used for free-surface capturing. Captive, semi-captive, and full 6DOF capabilities for multi-objects with parent/child hierarchy are available. A detailed description of the solver is given in Huang et al. [13] and references therein. Herein, blended k-ω/k-ε RANS turbulence model and level set free surface model are used. The 6DOF capabilities are used for the prediction of motions. Convection terms are approximated with finite differences second-order upwind. The second-order centered scheme is used for the viscous terms. The temporal terms are discretized using a second-order backwards Euler scheme. Incompressibility is enforced by a strong pressure/velocity coupling, achieved using either PISO or projection algorithms.

3.1.1 Computational Domain and Grids

For cases in calm water, the domain is in cylinder shape with the radius of 4.5L extending from z=-1L to z=0.25L in vertical direction. For cases in waves, the domain is in box shape extending from -0.5L<x<1.8L, -1.1L<y<1.1L, -1.0L<z<0.25L. The ship axis is aligned with x axis, with the bow at x=0 and the stern at x=1. The y-axis is positive to starboard with z pointing upward. The free surface at rest lies at z=0. The model is appended with skeg, twin bilge keels, rudders and rudder seats, struts, shafts and stabilizer fins. The propellers are modeled as a body force field applied at the position of propellers described by a disk volume. The computational grids are overset, with independent grids for the hull, appendages, refinement and background. The total number of grid points is 6.3-7.0M for calm water and 18.6 M for waves, decomposed into 72 and 181 for parallel processing, respectively. Details of the grids are shown in Figure 2.

3.1.2 Case Setup

The experimental conditions are followed as closely as possible in the simulations. In all cases, experimental data are used to impose the initial displacement, velocity, and acceleration. Mimicking the experimental procedures, all cases are run with constant propeller RPS, obtained by self-propulsion simulation at the corresponding Froude number. PID type feedback controllers are used for roll and heading for cases with active fins or rudders. The roll controller produce some angle for stabilizer fins using PD controller with P=0 and D=-5sec in full scale, same as experiment i.e. $\delta_F = -5\dot{\varphi}$ to put back the ship at upright position. The heading controller acts on rudder attempting to steer the ship at the desired heading. Since the heading controller was not recorded in experiment, a PD controller was employed

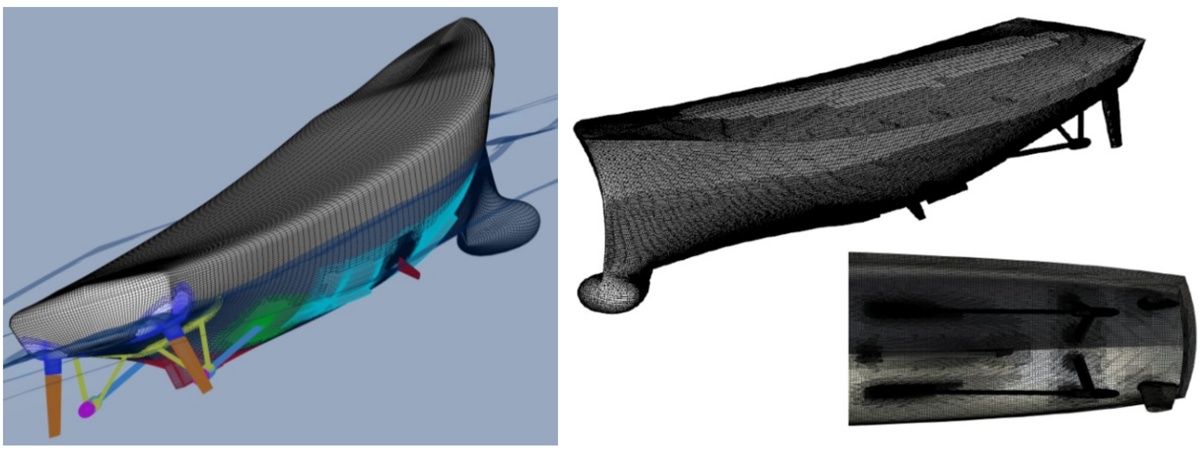

Figure 2: Overset grid system and instantaneous view of the free surface for CFDShip-Iowa (left) and unstructured grid system for ISIS-CFD (right)

with P and D estimated from fitting $\delta - \delta_0 = P(\psi - \psi_{target}) + D\dot{\psi}$ to experimental heading and rudder angle for each test. Due to the high cost per run, verification was not attempted.

3.2 ISIS-CFD

ISIS-CFD, developed by the CFD group of the Fluid Mechanics Laboratory and available as a part of the FINE^{TM}/Marine computing suite, is an incompressible unsteady Reynolds-averaged Navier Stokes (URANS) method. The solver is based on the finite volume method to build the spatial discretization of the transport equations. The unstructured discretization is face-based, which means that cells with an arbitrary number of arbitrarily shaped faces are accepted. A detailed description of the solver is given in e.g. Duvigneau and Visonneau [14]. The velocity field is obtained from the momentum conservation equations and the pressure field is extracted from the mass conservation constraint, or continuity equation, transformed into a pressure equation. In the case of turbulent flows, transport equations for the variables in the turbulence model are added to the discretization. Free-surface flow is simulated with a multi-phase flow approach: the water surface is captured with a conservation equation for the volume fraction of water, discretized with specific compressive discretization schemes discussed in Queutey and Visonneau [15]. The method features sophisticated turbulence models: apart from the classical two-equation k-w and k-e models, the anisotropic two-equation Explicit Algebraic Stress Model (EASM), as well as Reynolds Stress Transport Models are available. The technique included for the 6 degree of freedom simulation of ship motion is described by Leroyer and Visonneau [16]. Time-integration of Newton's laws for the ship motion is combined with analytical weighted or elastic analogy grid deformation to adapt the fluid mesh to the moving ship. Furthermore, the code has the possibility to model more than two phases. For brevity, these options are not further described here.

3.2.1 Computational Domain and Grids

The computational domain extends from -1.5L < x < 3.5L, -1.5L < y < 1.5L and -1.25L < z < 0.375L. The ship axis is located along x-axis with the bow located at x=0.5L and the stern at x=-0.5L. The free-surface at rest lies at z=0. The unstructured hexahedral grid is generated with HEXPRESS. All appendages are taken into account except the propellers, which are modeled as a body force field applied at the position of propellers. A local zone of refinement is created near the hull, to ensure small grid spacing. This grid is composed of 5.9 million cells with about 300,000 cells located on the hull. The local mesh distribution close to the bow and the stern is shown on the right-hand side of Figure 2.

3.2.2 Case Setup

The roll decay tests with no fins or passive fins are investigated. Firstly, an initial simulation with a ship free to move in trim and sinkage with no roll angle is carried out. For this simulation, the actuator disk theory is applied. Then, the initial roll angle is applied. The flow around the ship is computed by imposing the surge motion while all other modes of motion are free. Moreover, the rudder action due to the autopilot is ignored in these computations.

4 PF METHOD

4.1 FREDYN

Fredyn is developed by the Cooperative Research Navies (CRNAV) group. Its fundamentals are discussed in De Kat and Paulling [17]. The version considered in this paper is Fredyn version 10.3. Fredyn is a program dedicated to simulate the motions of high-speed semi-displacement ships in severe conditions. The program is intended to be used in the initial design stage when model test data are not available.

The mathematical model consists of a non-linear strip theory approach, where linear (wave radiation and diffraction) and non-linear (Froude-Krylov, including buoyancy) potential flow forces are combined with viscous forces (propeller, bilge keel, rudder and fin forces, hull lift and drag, roll damping, wind loads and etc). These viscous force contributions are of a nonlinear nature and based on (semi)empirical models. In the present work, the viscous forces are based on the default Fredyn model. The roll damping is based on an adapted method for fast displacement ships (FDS).

A recent application of Fredyn for the 5415M hull form in calm water and waves can be found in Carette and Van Walree [18] and Quadvlieg et al. [19]. Validation of amongst others roll damping predictions or motions in waves with Fredyn can be found in Boonstra et al. [20] and Levadou and Gaillarde [21]. The maneuvering prediction capability of Fredyn was validated by Toxopeus and Lee [1].

The hull form (sectional data) and the particulars of the propeller, bilge keels, rudders and stabilizer fins as described in Section 2.1 were used as input to the program. The bare hull resistance curve was based on an estimation using a modified version of the Holtrop and Mennen method [22]. This method also provides estimates of the propeller wake fraction and thrust deduction fraction. The propeller thrust curve was obtained from open water tests with the model propeller. Other than the use of the propeller open water tests and estimation of the resistance curve, wake fraction and thrust deduction fraction, all coefficients were based on the default values calculated by Fredyn. No additional tuning of the empirical coefficients based on model test data was conducted. The rudder seats were modeled as additional fixed rudders.

During the cases with the rudders steered by autopilot, the coefficients are determined from least-square fitting of the experimental rudder angle signal, see section 2.3. However, for simplification of the setup, the sway gain coefficient A was ignored. This means that deviations in the y position between the simulations and experiments can occur.

In Fredyn, the RPM of the propellers needs to be specified. In the present work, the RPM from the experiments was used as input. Due to a different balance of resistance and propeller thrust, this may result in a different speed during the simulation.

4.2 SWAN

SWAN2 2002 [23] is a 3D time-domain panel code developed at MIT. Details can be found in Sclavounos [24] and Kring et al. [25]. The software implements a fully 3D approach based on the distribution of Rankine sources over the wetted hull and the free surface. The linear free-surface condition is satisfied, while it has the capability of taking into account the non-linear Froude-Krylov and hydrostatic forces. This option however, was not activated in the present work.

A sensitivity analysis was conducted in order to define a suitable extent of the free surface grid in the longitudinal and lateral directions, as well as the respective number of panels fitted on the wetted surface of the vessel in both directions. The number of desired hull sheet nodes in a direction parallel to the X-axis is 30. The respective number of nodes on a direction perpendicular to X-axis is 8. The panel mesh extends on the free surface 0.5 L upstream, 1.5 L downstream and 1.0 L to the sides. A total of 2300 panels were fitted on the hull form and the free surface.

A time step of 0.05 sec has been used in the calculations. The simulated time history was 300 sec. The code can handle only passive fins providing also the variation of the angle of attack. The rudders are also handled as fins. Furthermore, in the use of SWAN2 an iterative procedure was added to converge to the actual dynamic draft and trim of the vessel at each speed. That pair of draft and trim was subsequently used in the unsteady calculations. In general, the linearity assumption and the fact that viscous roll damping is not taken into account reduces the reliability of the predictions in very high dynamic responses.

4.3 LAMP

LAMP (Large Amplitude Motions Program) is a 3D time-domain dynamic panel code. Forces due to viscous flow effects and other external forces such as hull lift, propulsors, rudders, etc. are modeled using other computation methods or with empirical or semi-empirical formulas. Calm water maneuvering is a special application of the general methodology, with no incident wave but retaining the wave-body interactions related to forward speed and ship motions. For a ship maneuvering in waves, either body linear or nonlinear hydrodynamic problems can be solved. The body nonlinear approach, which considers the effects of the ship's vertical motion relative to the calm water or incident wave, is usually used for the hydrostatic and Froude-Krylov wave forces. Details of the mathematical formulation, numerical implementation and application of LAMP for nonlinear seakeeping or maneuvering problems can be found in e.g. Yen et al. [2][26] and Lin et al. [27][28].

A sensitivity study was carried out to determine the computation domain and grid size. To get stable and converged results, 1388 hydrodynamic body panels were used on the wetted portion of the hull and skeg and 2208 panels were used on a local portion of the free surface. The free surface domain extends from 1L upstream and 1L downstream in the longitudinal direction, and extends 1.5L to the starboard and to the port sides of the ship centerline.

The procedure to derive LAMP's maneuvering forces coefficients was developed and validated for participation in the SIMMAN 2008 Workshop and is described in Yen et al. [2]. The PMM tests for the workshop were performed at MARIN using an appended model with the propeller rotating at the model self-propulsion point. LAMP's hull lift model and higher-order damping coefficients were adjusted to fit the measured forces and moments from the PMM test. The bilge keels, rudder, and stabilizing fins were modeled as low aspect ratio lifting surfaces and adjusted to match the measured forces from the PMM tests. The lift of the skeg was modeled as an additional low aspect ratio lifting surface. The open-water propeller thrust curve, wake fraction and thrust deduction, and the velocity increment on rudder inflow due to propeller wash were also modeled from descriptions and data in the test report.

The 6DOF time-domain simulations were carried out for each of the test cases. The LAMP simulations were done at model scale and then converted to full scale for presentation. The propeller RPM for each run was set to achieve the initial, calm-water speed from the experiment and was held constant for the simulation. LAMP's autopilot, which implements a slightly different algorithm than the autopilot in the experiment, uses the experimental values of *P*, *D*, and *A*, but does not include the rudder bias (δ_0). For small course errors, LAMP's algorithm behaves almost exactly like the one for the experiment.

5 SB METHOD

5.1 SurSim and FreSim

SurSim and FreSim are basically the same programs, but with different implementations of the hull forces and rudder/fin forces. All other aspects are modeled using shared libraries. SurSim is dedicated to the simulation of the maneuverability of mainly twin-screw ferries, cruise ships and motor yachts, while FreSim is used for high-speed semi-displacement ships. Both codes model the motions of the ship in four degrees of freedom. SurSim and FreSim do not contain wave modeling and therefore they cannot be applied to study the course keeping of ships in waves. The programs are of the modular type, i.e. forces on each component of the ship are modeled separately. Both models utilize cross flow drag coefficients (see e.g. Hooft [29]) to model non-linear effects in the forces and moments on the ship. The linear maneuvering coefficients are estimated using the slender body method described by Toxopeus [30]. More information about SurSim and FreSim and their validation can be found in Toxopeus and Lee [1]. For maneuvering predictions, FreSim is mostly applicable to slender naval ships, while SurSim is mostly applicable to ships of moderate L/B ratio and moderate block coefficients.

In SurSim and FreSim rudders and fins are modeled as lifting surfaces, treating fins as "rudders" without propeller in front. The forces and moments generated by the lifting surfaces are all added in the output files and therefore the forces generated by the rudders cannot be separated by the forces generated by the fins. In this paper, based on the type of test, it was decided to attribute the full loads generated by all lifting surfaces as rudder loads, or as fin loads. In some cases in which both the rudders and the fins generate large forces, disagreement from the loads found during the experiments or in the results from other methods can be expected. Furthermore, bilge keel forces are included in the hull forces and cannot be analyzed separately.

For the setup of the cases (roll decay and forced oscillation) identical input parameters were used for SurSim, FreSim and Fredyn, except for the setting of the propeller RPM. In SurSim and FreSim, the RPM was determined by the program while in Fredyn the RPM value was taken from the measurements. See section 4.1 for more details of the setup.

Table 3: The period and damping coefficients for roll decay

Type	Parameters	EFD	CFDShipIowa (E%D)	ISIS-CFD (E%D)	Fredyn (E%D)	LAMP (E%D)	Swan2 (E%D)	FreSim (E%D)	SurSim (E%D)
No fins	$T_{\phi d}$ (s)	11.1	11.2 (-0.9)	11.9 (-7.2)	11.7 (-5.4)	11.4 (-2.7)	12.2 (-9.9)	12.3 (-10.8)	11.6 (-4.5)
	α (MNms/rad)	68.1	61.1 (10.3)	40.7 (40.2)	59.9 (12.0)	75.4 (-10.7)	52.5 (22.9)	71.1 (-4.4)	58.8 (13.7)
	β (MNms^2/rad^2)	4.28	1.65 (61.4)	6.64 (-55.1)	2.41 (43.7)	1.17 (72.7)	0.62 (85.5)	3.54 (17.3)	4.70 (-9.8)
Passive fins	$T_{\phi d}$ (s)	11.3	11.3 (0.0)	11.9 (-5.3)	11.7 (-3.5)	11.5 (-1.8)	12.2 (-8.0)	12.5 (-10.6)	11.7 (-3.5)
	α (MNms/rad)	69.0	65.9 (4.5)	45.0 (34.8)	74.9 (-8.6)	96.3 (-39.6)	56.1 (18.7)	80.3 (-16.4)	67.8 (1.7)
	β (MNms^2/rad^2)	14.4	16.1 (-11.8)	12.9 (10.4)	-0.003 (100)	-3.1 (121)	0.49 (96.6)	4.3 (70.1)	4.9 (66.0)
Active fins	$T_{\phi d}$ (s)	12.2	12.4 (-1.6)	-	11.5 (5.7)	11.7 (-4.1)	-	12.8 (-4.9)	12.0 (1.6)
	α (MNms/rad)	202.4	89.3 (55.9)	-	151.2 (25.3)	147.4 (27.2)	-	128.6 (36.5)	95.0 (53.1)
	β (MNms^2/rad^2)	20.8	22.4 (-7.7)	-	-19.8 (195)	3.7 (82.2)	-	7.1 (65.9)	19.1 (8.2)

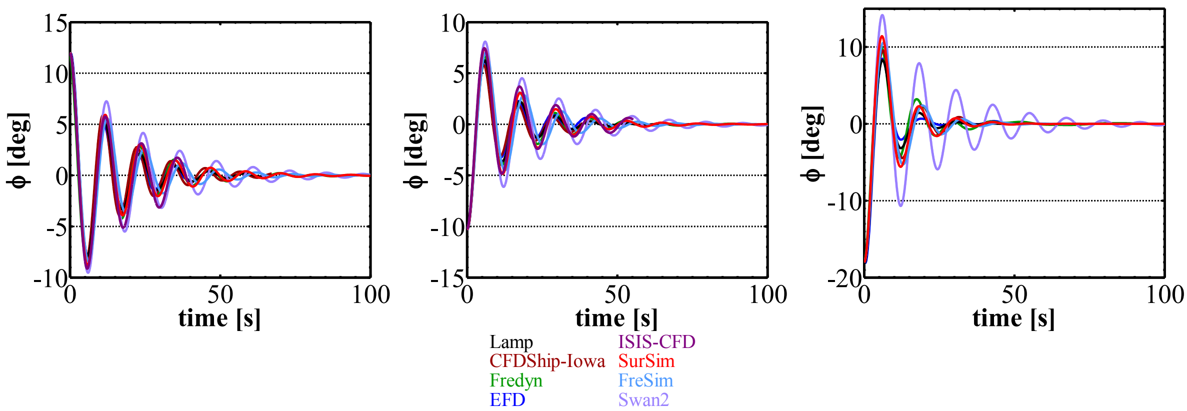

Figure 3: Roll decay: without fins (left), passive fins (middle), active fins (right)

6 COMPARISON CFD, PF, AND SB METHODS

6.1 Data Analysis Method

For roll decay cases, the roll damping coefficients are derived based on Himeno Method (Himeno [31]) to study the effects of the stabilizer fins. In this method, it is assumed that the roll motion can be described by the following 1DOF equation:

$$(I_{xx} + m_{xx})\ddot{\varphi} + \alpha\dot{\varphi} + \beta|\dot{\varphi}|\dot{\varphi} + mgGM\varphi = 0 \quad (1)$$

Here I_{xx} is moment of inertia around x axis, m_{xx} is added inertia, α and β are linear and quadratic damping coefficients, m is ship mass and GM is metacenteric height.

For forced roll in calm water and wave cases, the mean, n-th harmonic amplitude and phase of any motion are determined from time histories using Fourier decomposition.

The damping coefficients for roll decay in calm water and harmonics for forced roll in calm water and wave cases are compared with EFD data and the difference between data *D* and simulation values *S* (error) is reported as *E%D = (D-S)%D*.

6.2 Roll Decay in Calm Water

Table 3 and Figure 3 show the results for the roll damping cases. During the tests, the model is given an initial roll angle, which subsequently damps quickly such that the roll amplitude decreases to less than a deg in four cycles. Without fins, the damped roll period is about $T_{\phi d}$=11.1 sec (close to hydrostatic natural roll period $T_{\phi h}=\frac{2\pi k_{xx}}{\sqrt{gGM}}=10.95$ s). The damped roll period with passive fins is about $T_{\phi d}$=11.3 s in all cycles, about 2% larger than the period of the model with no fins. With active fins the damping is significantly larger such that the roll is reduced to 2 deg after only one cycle and reaches to less than a degree for the rest of the test. The damped roll period increases to about 12.2 s.

The passive fins increase the non-linear damping by 230% compared with the case with no fin while the linear damping is similar. The active fins result in a three times larger linear damping and a 45% larger non-linear damping.

Comparing all the computed motions with the EFD data shows that most CFD, PF and SB methods predict the roll decay time history fairly well. The effects of passive or active stabilizing fins is reasonably well predicted by all methods.

For the case without fins or with passive fins, the roll period is over-predicted by up to 10.8%D. Generally, the largest errors are found for the SB methods and the smallest ones for the CFD methods. With active fins, the prediction of the period is closer to the experimental one and within 6%D.

The prediction errors for the linear and quadratic damping coefficients are up to 40%D and 9.8-85%D, respectively. The smallest comparison errors in the coefficients are found for the CFD methods. Therefore, high-fidelity methods such as CFD appear to predict much better the nonlinearities and complex physics associated with roll decay. It should be noted that in PF and SB methods the viscous roll damping, which is caused by hull friction and eddies generated by hull, bilge keels and other appendages, is modeled, not solved. Furthermore, errors in the linear damping coefficient can be compensated by errors in the non-linear one. In the SWAN2 predictions only the wave and lift damping was modeled and the viscous damping was not included. Furthermore, the fins were not set to active mode. Therefore large comparison errors are found.

6.3 Forced Roll in Calm Water

6.3.1 Rudder Induced Roll with Passive Fins

The results for rudder-induced roll with passive fins are shown in Table 4 and Figure 4. The roll response shows only first harmonic oscillations at T_R with amplitude of 0.464δ due to the first order rudder/yaw and roll coupling. The yaw motion oscillates mainly at T_R with amplitude of 0.018δ and 236 deg phase lag with rudders due to the ship inertia and lethargy.

Table 4: FFT of ship motions and rudder angle for forced roll induced by rudders with passive fins

	EFD			CFDShip-Iowa			Fredyn			LAMP			FreSim			SurSim		
value	a_1	a_2/a_1	phase	a_1 E%D	a_2/a_1 E%D	phase E%2π	a_1 E%D	a_2/a_1 E%D	phase E%2π	a_1 E%D	a_2/a_1 E%D	phase E%2π	a_1 E%D	a_2/a_1 E%D	phase E%2π	a_1 E%D	a_2/a_1 E%D	phase E%2π
δ	13.4	0.003	0	-4.5	0	0	-11.9	0	0	-6.5	0	0	-10.2	0	0	-10.2	0	0
ϕ/δ	0.464	0.001	137	-30	0	5.6	-58.2	0	10.8	-6.3	0	5.8	-13.5	0	11.1	-41.9	0	0.8

Table 5: FFT of ship motions and rudder angle for forced roll induced by rudders with active fins

	EFD			CFDShip-Iowa			Fredyn			FreSim			SurSim		
value	a_1	a_2/a_1	phase	a_1 E%D	a_2/a_1 E%D	phase E%2π	a_1 E%D	a_2/a_1 E%D	phase E%2π	a_1 E%D	a_2/a_1 E%D	phase E%2π	a_1 E%D	a_2/a_1 E%D	phase E%2π
δ	13.43	0.002	0	-4.2	0	0	-11.6	0	0	-10.0	0	0	-10.0	0	0
δ_F/δ	0.737	0.009	27	-34.3	0	1.7	-92.0	0	6.9	-34.3	0	5.3	-60.5	0	-1.9
ϕ/δ	0.274	0.004	132	-34.2	0	5.3	-93.4	0	8.9	-35.8	0	7.8	-62.4	0	0.6

Table 6: FFT of ship motions and rudder angle for forced roll induced by fins

	EFD			CFDShip-Iowa			Fredyn			LAMP			FreSim			SurSim		
value	a_1	a_2/a_1	phase	a_1 E%D	a_2/a_1 E%D	phase E%2π	a_1 E%D	a_2/a_1 E%D	phase E%2π	a_1 E%D	a_2/a_1 E%D	phase E%2π	a_1 E%D	a_2/a_1 E%D	phase E%2π	a_1 E%D	a_2/a_1 E%D	phase E%2π
δ_F	25.48	0	0	1.8	0	0	1.8	0	0	1.9	0	0	2.4	0	0	2.4	0	0
δ/δ_F	0.01	0.075	18	25.2	0.1	-81.7	NA	NA	NA	-231.6	0	-0.3	NA	NA	NA	NA	NA	NA
ϕ/δ	0.252	0.002	300	13.0	0	3.6	39.6	0	7.5	24.3	0	4.7	41.5	0	12.2	31.6	0	3.1

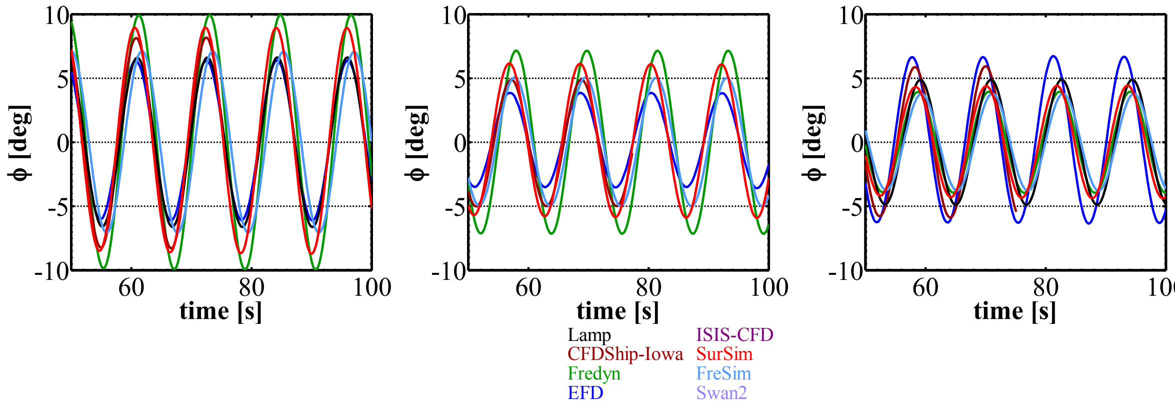

Figure 4: Forced roll: rudder, passive fins (left), rudder, active fins (middle), fins (right)

The first order coupling of sway motion with yaw causes harmonic oscillations on side motions with amplitude of 0.24 m at T_R..

All numerical methods show roll oscillations at T_R. However, the roll amplitude is over predicted by all of the methods with E=6-58%D suggesting under prediction of roll damping and/or over prediction of roll moment due to the rudder action. Fredyn has the maximum over-prediction while the best agreement is for LAMP as the damping could be tuned properly to EFD value. The roll phase is also predicted within E=0.8-10.8%2π.

6.3.2 Rudder Induced Roll with Active Fins

Table 5 and Figure 4 show the results for forced roll motion induced by rudders while the fins are active to control the roll motion. The forced rudder motions induce roll oscillations at T_R with the amplitude of 3.68 deg, compared to 6.216 deg roll amplitude for previous test with passive fins. The fins are controlled by $\delta_F = -5\dot{\varphi}$ and therefore the peaks for the fin angles with a value of about 10 deg occur when the roll is zero and the magnitude of roll rate is at maximum.

The roll motion in the simulations is over predicted for all methods within E=34-93%D with maximum error for Fredyn and minimum error for CFDShip-Iowa. Fredyn also shows large errors for the roll phase. The fin angles are over predicted as well since the fin angles are correlated with roll angle.

6.3.3 Fins Induced Roll

Unlike the two previous cases where the roll was induced by forced rudder motion, the forced roll motion can be provided by moving the fins under forced harmonic motion. Table 6 and Figure 4 show the EFD and numerical results for forced roll induced by fins. The oscillatory motion of the fins creates a roll motion with amplitude of 6.43 deg and 60 deg phase lag with the fin motion.

The roll angle amplitude as computed by the numerical tools is under predicted by all methods with E=13-42%D with maximum/minimum error of FreSim and CFDShip-Iowa, respectively. The phase difference between roll and fin motions is under predicted by all methods, with the largest errors found for FreSim and Fredyn with E>7%D.

6.4 Seakeeping in Waves

6.4.1 Regular Head Waves with Active Fins

The results of the case of seakeeping in regular head waves are shown in Table 7 and Figure 5. The ship is located in a wave with amplitude of 1.03 m and frequency of 0.6 rad/s (λ=1.206L) indicating linear wave with wave slope of Ak=0.0378. The roll motion oscillates with very small angle (<0.8 deg) due to nearly zero heading of the ship in the waves, as shown in Figure 5. The fins turn based on the roll rate to control the roll motion. However, the fin angles are quite small and are less than 2 deg as the roll response is negligible in head waves. Both pitch and heave show large oscillations at T_e due to linear wave induced heave force/pitch moment and heave/pitch linear coupling. The pitch motion shows oscillation with amplitude of 1.75 deg (0.8Ak). The heave shows oscillations with amplitude and mean value of 0.78m and -0.19 m, respectively. The surge motion shows same harmonics as heave and pitch, which causes oscillations on surge velocity. The averaged surge velocity is about 8.95 m/s compared to the desired speed of 9.56 m/s. This is the result of the added resistance induced by waves.

Table 7: FFT of ship motions and rudder and fin angles for regular head waves, A=1.03m, Ak=0.0378

	EFD			CFDShip-Iowa			Fredyn			LAMP			SWAN2		
value	a1	a2/a1	phase	a1 E%D	a2/a1 E%D	phase E%2π	a1 E%D	a2/a1 E%D	phase E%2π	a1 E%D	a2/a1 E%D	phase E%2π	a1 E%D	a2/a1 E%D	phase E%2π
x/A	19.34	0.498	7	1.7	0.5	1.4	-2.6	0.5	1.4	2.7	0.5	-98.1	1.3	0.5	1.4
z/A	0.753	0.008	56	-1.3	0	-82.5	0.8	0	-82.2	-25.6	0	15	4.9	0	15.6
θ/Ak	0.808	0.008	274	-7.6	0	15.3	10.5	0	13.6	-4.1	0	15.3	3.3	0	15

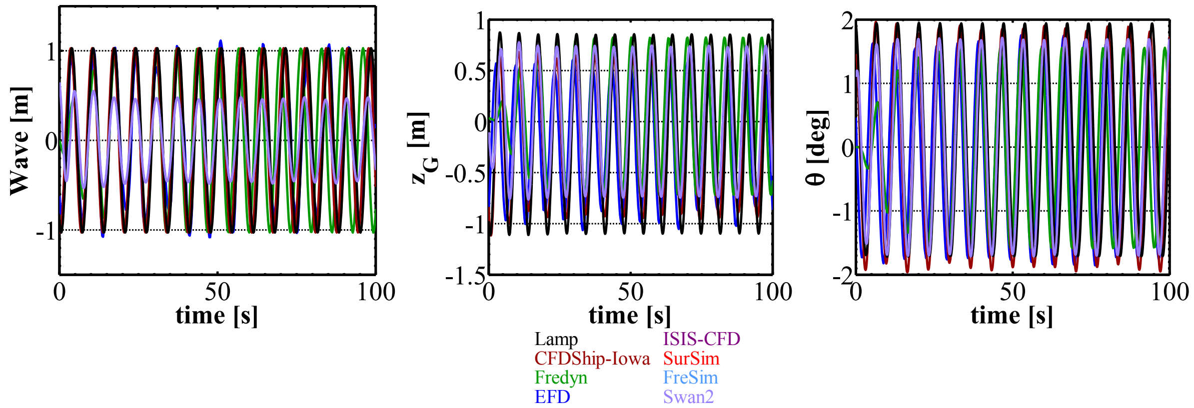

Figure 5: Regular head waves, A=1.03m, Ak=0.0378

The results for the different prediction methods are also shown in Table 7 and Figure 5. Note that SB methods could not be used for wave cases, as their mathematical models are only suitable for calm water. Also, ISIS-CFD is not used and the rudders and fins are passive for SWAN2 simulations. In addition, the roll and yaw motions (as well as dynamic fin and rudder) are not considered in Fredyn and LAMP computations since the ship is assumed to sail in head waves while CFDShip-Iowa and SWAN2 computations consider the small wave heading and they predict roll and yaw motions. The time history of the wave shows that all methods follow EFD in terms of phase and period except Fredyn as the ship speed is over predicted and encounter period is under predicted. This is caused by an unbalance of the given RPM and the corresponding ship speed. The amplitude of pitch motion is quite well predicted by all methods, with largest error of 11%D by Fredyn. The phase of pitch motion is not predicted well for all methods showing about 50 deg phase lag. For heave motion, the mean value is well predicted for all methods. The comparison error in heave amplitude is within 5%D, except for LAMP, for which an over prediction of 26%D is found. The results show about 60 deg phase lag for all heave predictions compared with EFD data.

6.4.2 Regular Beam Waves with Active Fins

The EFD results for seakeeping in regular beam waves are shown in Table 8 and Figure 6. The wave amplitude is 0.96 m and the wave frequency is 0.8 rad/sec (λ=0.678L) i.e. linear wave condition with Ak=0.0626. The wave approaches the ship from starboard. The roll time history shows the ship rolls to starboard at max angle all the time when the wave trough is located at the ship center of gravity. Similarly, the max roll to portside happens when the

Table 8: FFT of ship motions and rudder and fin angles for regular beam waves, A=0.96m, Ak=0.0626

	EFD			**CFDShip-Iowa**			**Fredyn**			**LAMP**			**SWAN2**		
value	**a1**	**a2/a1**	**phase**	**a1**	**a2/a1**	**phase**	**a1**	**a2/a1**	**phase**	**a1**	**a2/a1**	**phase**	**a1**	**a2/a1**	**phase**
				E%D	E%D	E%2π	E%D	E%D	E%2π	E%D	E%D	E%2π	E%D	E%D	E%2π
δ/Ak	0.325	0.047	151	11.2	0.1	-18.6	-161.6	0	-12.2	-331.1	0	-1.7	NA	NA	NA
δ_F/Ak	2.833	0.001	25	31.2	0	-1.1	44.6	0.1	-7.5	21	0	-5.3	NA	NA	NA
x/A	24.448	0.499	10	-0.7	0.5	1.7	-4.5	0.5	-96.4	2.1	0.5	2.8	1.5	0.5	-96.9
y/A	0.717	0.02	266	-8.6	0	-2.5	3.8	0	-3.6	5.1	0	-2.2	4.2	0	-10.3
z/A	1.061	0.002	345	-1	0	-1.7	13.7	0	-3.1	-2.5	0	-3.9	7	0	95
ϕ/Ak	0.71	0.002	137	31.4	0	4.2	44.8	0	-1.4	21.2	0	0.8	30.4	0	17.5
θ/Ak	0.025	0.182	121	9.1	0.1	-3.3	-202.3	0	-56.1	25	0.1	-3.1	-38.6	0	-64.4
ψ/Ak	0.025	0.052	306	6.7	0.1	-0.8	-91	0	7.5	-70.8	0	-6.1	-78.7	0	6.7

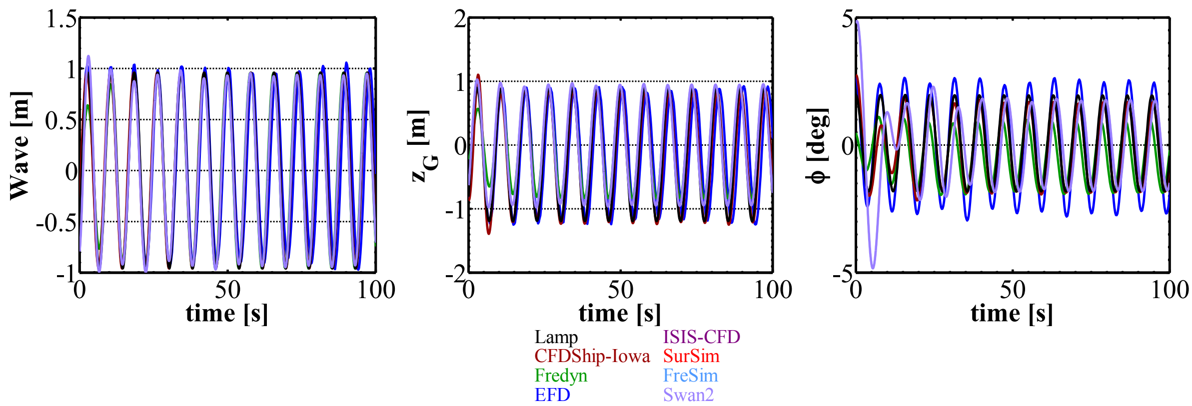

Figure 6: Regular beam waves, A=0.96m, Ak=0.0626

wave crest is located at ship center of gravity. The roll period is 7.85 sec corresponding to wave frequency T_e. The roll amplitude is about 2.5 deg (0.71Ak) and the mean value is nearly zero. The roll is under the control of the fins such that the fins turn 10 deg to damp the roll motion. The sway and yaw motions show harmonic response at T_e with amplitude of 0.7A and 0.09 deg, due to linear wave-induced sway force/yaw moment and/or linear coupling of roll, sway and yaw. The surge, heave and pitch motion shows harmonic oscillation with same period as wave, due to linear wave induced surge force/heave force/pitch moment and/or linear coupling of heave and pitch. The pitch amplitude is 0.088 deg (0.025Ak) and it is in phase with roll motion. The heave oscillates with amplitude of 0.97 m (1.06A) and it is again nearly in phase with wave at center of gravity. Note that the ratio of wavelength and ship beam size is 5.05 and the ship just moves up and down with the wave. The surge velocity is about 9.3 m/s very close to the value in calm water. The rudder angle shows harmonics at wave frequency as it is correlated with yaw motion.

The results for different predictions shown in Figure 6 indicate that the generated waves follow closely the experimental data in terms of the amplitude and phase. The roll motion shows that all methods under predict the roll amplitude with E=21-45%D. The best agreement is for LAMP and the largest under prediction is for Fredyn, as shown in Table 8. The roll phase is predicted within E=0.8-17%D with the largest error for SWAN2. Since the roll is under predicted, the fin angle is also under predicted by all methods. The yaw motion shows oscillations at T_e for all prediction methods while the amplitude is over predicted by PF methods with E>70%D compared to E=6.7%D for the CFD method, showing that the yaw damping is not properly modeled in PF methods. In addition, the trend of yaw motion (mean value) is not predicted by PF methods. The amplitude of oscillations at T_e is predicted for side motion by all methods but the mean value and the trend is only well predicted by CFDShip-Iowa. For pitch response, the amplitude is predicted fairly well by CFDShip-Iowa (E=9%D) while all PF methods show large errors with E>25%D. The pitch phase is not predicted well by Fredyn and SWAN2 while CFDShip-Iowa and LAMP show E=3%D. For heave amplitude, PF methods show E=2.5-14%D while CFDShip-Iowa prediction has an error with E=1%D. The ship speed is quite constant and close to EFD value for all methods except Fredyn, which shows an increase of speed during the run, due to the imbalance of propeller thrust and resistance as before. The rudder angle amplitude shows large errors for PF methods particularly for Fredyn as it is correlated with yaw motion.

6.4.3 Stern-Quartering Bi-Chromatic Waves with Active Fins

The EFD results for seakeeping in bi-chromatic waves are shown in Figure 7. The bi-chromatic wave consists of two regular waves with same amplitude of 1.77 m and periods of 9.4 sec (k=0.0455 m^{-1}) and 10.2 sec (k=0.03868 m^{-1}). The wave heading is 120 deg with respect to the ship bow and approaches the ship from portside. The bi-chromatic wave envelope has oscillations at both high frequency and low frequency. The low frequency oscillations have a nominal wavelength of $\lambda = \frac{4\pi}{\Delta k}$ = 12.97L and nominal period of $T = \frac{4\pi}{\Delta\omega}$ = 239.7 sec. The high frequency oscillations occur at $T = \frac{4\pi}{\omega_1+\omega_2}$ = 9.78 sec. The recorded EFD wave shows both harmonics but at encounter periods due to the ship speed. The roll motion shows both harmonics as well and is fairly in phase with wave amplitude at center of gravity. The max roll angle happens for max wave height and it is about 20 deg for roll to starboard and 15 deg for roll to portside. The fin motions are correlated with roll as $\delta_F = -5\dot{\varphi}$. The large roll rate causes the fin angle to reach their maximum of 25 deg during the test. The yaw motion also shows oscillations induced by the wave moment. The maximum amplitude of yaw fluctuations happens when the wave amplitude is at maximum and it is about 3.5 deg. The pitch response is similar to roll but has about 180 deg phase lag with waves. The max pitch is near 3 deg and happens when the ship is located on the wave trough or wave crest. The heave motion shows oscillations at both low and high frequency similar to pitch motion but has 90 deg phase lag with pitch as it was expected. The maximum heave motion is 2.5 m, 40% of the design draft, which is very large. The surge motion and consequently the surge velocity show both harmonics. The surge velocity oscillates with maximum amplitude of 1m/s for maximum wave height. The oscillations on yaw motion create fluctuations on rudder angles as they are defined based on PID controller on the heading. The maximum rudder fluctuation has amplitude of 22.5 deg and it is for max yaw amplitude.

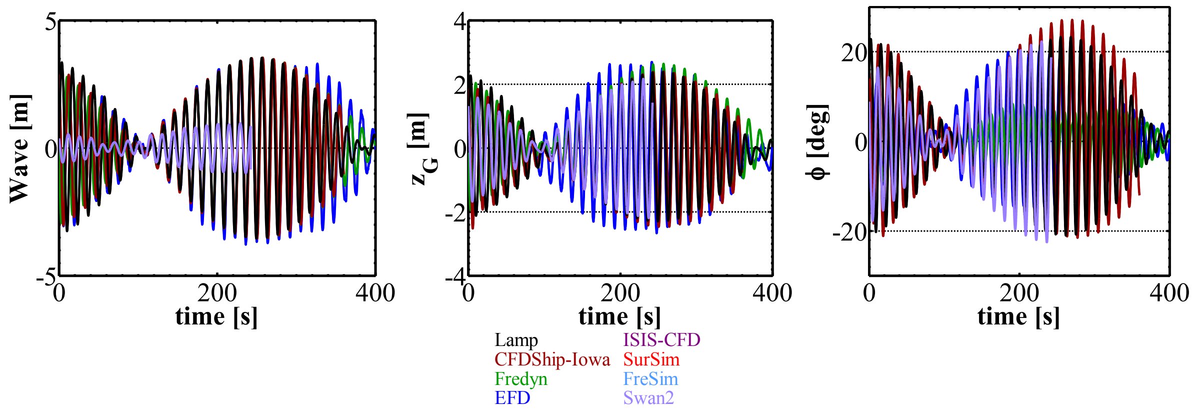

Figure 7: Stern-quartering bi-chromatic waves

The predictions for different methods are shown in Figure 7 as well. The wave at center of gravity shows a phase lag with EFD for most predictions due to differences in ship speed. The predictions for roll show LAMP, SWAN2 and CFDShip-Iowa over predict the roll angle but Fredyn under predicts the roll considerably. Since fin angle prediction is correlated with roll motion prediction, the fin angles are over predicted by all methods except Fredyn. The amplitude of oscillations is predicted for side motion using all methods but the mean value and the trend is only well predicted by CFDShip-Iowa. The yaw motion shows good agreement for CFDShip-Iowa while Fredyn over predicts the yaw oscillations amplitude and LAMP under predicts that. For pitch and heave motions, good agreement is observed for all methods. The rudder angle prediction is dependent on yaw motion prediction such that the agreement for LAMP and Fredyn predictions are not good. The surge motion and velocity prediction show some differences with EFD. The amplitude of surge velocity oscillations are under predicted by most of methods with largest errors for PF methods.

7 CONCLUSIONS

SB, PF, and CFD free running simulations were performed for 5415M in calm water and waves and compared against available experimental data. A detailed validation study was conducted for the motions of the ship and controllers.

The studies showed that both roll decay and forced roll induce oscillations on yaw motion, which turn the ship away from the target heading and activate the rudders to keep the ship at the desired course. It is shown that the passive and active fins reduce the roll amplitude by increasing linear and nonlinear roll damping. For wave cases, EFD data showed oscillations at wave encounter frequency on motions. The amplitude of motions was very large for bi-chromatic waves. The measured loads on the fins, rudders and bilge keels showed the contribution of the appendages on the ship responses.

The SB methods (FreSim and SurSim) were only applied for roll decay and forced roll in calm water. For roll decay in calm water, the roll motion was predicted reasonably well. The largest errors were found for the case with active fins. For forced roll cases, SB could predict the harmonics induced on ship motions by forced rudder or fins but often showed quite large errors for the amplitudes, especially for the forced fins case.

The PF methods (Fredyn, LAMP and SWAN2) were validated for roll decay and forced roll in calm water and seakeeping in waves. For roll decay in calm water, the roll period was predicted with average of E=4.6%D. The linear roll damping coefficients were predicted with average of E=26%. For nonlinear damping, all PF methods show large errors (E~ 97%D) suggesting that nonlinearities are not fully considered in PF methods. The roll induced harmonics were often well predicted on sway and yaw but not on heave and pitch i.e. it is challenging for PF methods to consider the higher order coupling between roll, heave and pitch. For forced roll cases, roll showed large 1st harmonic amplitude similar to EFD for all codes with average of E=44%D. All PF methods showed large sway and yaw 1st harmonic amplitude, similar to EFD. However, the amplitude was not predicted well suggesting the viscous damping terms are not tuned. For heave and pitch, PF codes showed the second harmonics but with large errors E=112%. The PF methods in waves predicted quite well the amplitude of oscillations on most of motions but often showed large errors for the mean values and phases. Overall, LAMP showed the best results of all PF codes, indicating that a-priori tuning of PF codes using PMM results or experiments improves the predictive capability of the tool considerably.

Among CFD methods, ISIS-CFD was only used for roll decay with no and passive fin while CFDShip-Iowa is validated for all cases. For roll decay cases, the roll period was predicted with on average a smaller error than the SB and PF predictions. The linear roll damping was predicted with same order error as PF codes with tuned damping terms but the nonlinear damping showed much better agreement with EFD data. Therefore, only high fidelity CFD is capable of accurately simulating the physics associated with roll decay. The good prediction of roll and nonlinearities also resulted in good predictions for other motions including heave and pitch. For forced roll cases, CFD could predict same harmonics as EFD for all motions. The roll amplitude was better predicted compared with SB and PF methods. The other motions are often predicted with less error compared with PF and SB. In particular, the predictions are much better for second harmonics amplitudes on heave and pitch. For wave cases, the amplitude and phase of the oscillations on most motions were again predicted better than PF methods.

For future work, the local flow field provided by CFD simulations will be investigated to study the interaction of vortical structures produced by the fins and other appendages. The flow physics could provide better understanding of fins and bilge keels efficiencies in vicinity of other appendages. Potential flow and CFD simulations are currently being performed in irregular waves to evaluate the seakeeping and course keeping performance of the ship in random seas in collaboration with NATO AVT-216.

ACKNOWLEDGEMENTS

The research performed at IIHR was sponsored by the US Office of Naval Research grant N000141010017 under administration of Dr. Thomas Fu. The CFD simulations were conducted utilizing DoD HPC. The authors gratefully acknowledge the permission given by the Danish, Italian and Netherlands Navies to use the test results obtained within Supplement Joint Program 10.111 to the Western European Armaments Group Memorandum of Understanding for THALES.

REFERENCES

[1] Toxopeus S.L. and Lee S.W. (2008), Comparison of maneuvering simulation programs for SIMMAN test cases, SIMMAN 2008 Workshop on Verification and Validation of Ship Maneuvering Simulation Methods, pages E56-61, Copenhagen, Denmark, April 2008.

[2] Yen T.G., Liut D.A., Zhang S., Lin W.M., and Weems K.M. (2008), LAMP Simulation of Calm Water Maneuvers for a US Navy Surface Combatant, SIMMAN 2008, Copenhagen, Denmark.

[3] Bunnik T.H.J., Daalen E.F.G. van, Kapsenberg G.K., Shin Y., Huijsmans R.H.M., Deng G, Delhommeau G., Kashiwagi M. and Beck B. (2010), A comparative study on state-of-the-art prediction tools for seakeeping, 28th Symposium on Naval Hydrodynamics, Pasadena, California, 12-17 September.

[4] Stern F., Agdrup K., Kim S.Y., Cura Hochbaum A., Rhee K.P., Quadvlieg F.H.H.A., Perdon P., Hino T., Broglia R. and Gorski J. (2011), Experience from SIMMAN 2008-The First Workshop on Verification and Validation of Ship Maneuvering Simulation Methods, Journal of Ship Research, Vo. 55, pp. 135-147.

[5] Sadat-Hosseini H., Carrica P.M., Stern F., Umeda N., Hashimoto H., Yamamura S., Mastuda A. (2011a), CFD, system-based and EFD study of ship dynamic instability events: surf-riding, periodic motion, and broaching, Journal of Ocean Engineering, Vol. 38, Issue 1, pp. 88-110.

[6] Sadat-Hosseini, H., Araki M., Umeda N., Sano M., Yeo D. J., Toda Y., Stern F., (2011b), CFD, system-based method, and EFD investigation of ONR tumblehome instability and capsize with evaluation of the mathematical model, 12th International Ship Stability Workshop, pp.135-145.

[7] Carrica P.M., Sadat-Hosseini H., Stern F. (2012), CFD Analysis of Broaching for a Model Surface Combatant with Explicit Simulation of Moving Rudders and Rotating Propellers, Computer & Fluids, Vol. 53, pp. 117-132 .

[8] Sadat-Hosseini H., Wu P.C., Carrica P.M., Stern F. (2014), CFD simulations of KVLCC2 maneuvering with different propeller modeling, Proceedings of the SIMMAN2014 workshop.

[9] Araki, M., Sadat-Hosseini, H., Sanada, Y. Tanimoto, K., Umeda, N., and Stern, F. (2012a), Estimating Maneuvering Coefficients Using System identification Methods with Experimental, System-based, and CFD Free-running Trial Data, Ocean Engineering, Vol. 51, pp. 63-84.

[10] Araki, M., Sadat-Hosseini, H., Sanada, Y., Umeda, N., and Stern, F. (2012b), Study of System-based Mathematical Model using System Identification Method with Experimental, CFD, and System-Based Free-Running Trials in Wave, Proceedings of the 11th International Conference on the Stability of Ships and Ocean Vehicles, Athens, Greece, Sept 23-28.

[11] Toxopeus S.L. (2011), Practical application of viscous-flow calculations for the simulation of manoeuvring ships, PhD thesis, Delft University of Technology, ISBN 978-90-75757-05-7.

[12] Toxopeus, S.L., Walree F. van, and Hallmann R. (2011), Maneuvering and Seakeeping Tests for 5415M. AVT-189 Specialists' Meeting, Portsdown West, UK.

[13] Huang J., Carrica P., Stern F. (2008), Semi-coupled air/water immersed boundary approach for curvilinear dynamic overset grids with application to ship hydrodynamics, International Journal Numerical Methods Fluids, Vol. 58, pp. 591-624.

[14] Duvigneau R., Visonneau M. and Deng G.B. (2003), On the role played by turbulence closures in hull shape optimization at model and full scale. Journal of Marine Science and Technology, Vol. 8, pp. 11-25.

[15] Queutey P. and Visonneau M. (2007), An Interface Capturing Method for Free-Surface Hydrodynamic Flows, Computers & Fluids, Vol 36, No. 9, pp. 1481–1510.

[16] Leroyer A. and Visonneau M. (2005), Numerical methods for RANSE simulations of a self-propelled fish-like body, J. Fluid & Structures, Vol. 20, No. 3, pp. 975–991.

[17] De Kat, J. O., and Paulling J. R. (2001), Prediction of extreme motions and capsizing of ships and offshore marine vehicles, 20th International Conference on Offshore Mechanics and Arctic Engineering (OMAE), paper number OMAE2001/OFT-1280, Rio de Janeiro, Brazil, June.

[18] Carette N. F. and Walree F. van (2010), Calculation method to include water on deck effects, 11th International Ship Stability Workshop (ISSW), pp. 166-172, Wageningen, The Netherlands, June.

[19] Quadvlieg F.H.H.A., Armaoğlu E., Eggers R., and Coevorden P. van (2010), Prediction and verification of the maneuverability of naval surface ships. SNAME Annual Meeting and Expo, Seattle/Bellevue, WA, November.

[20] Boonstra H., Jongh M. P. de, and Pallazi L. (2004), Safety assessment of small container feeders. 9th Symposium on Practical Design of Ships and Other Floating Structures (PRADS), Lübeck-Travemünde, Germany, September.

[21] Levadou M. and Gaillarde G. (2003), Operational guidance to avoid parametric roll, RINA - Container vessels Conference.

[22] Holtrop J. and Mennen G.G.J. (1982), An Approximate Power Prediction Method. International Shipbuilding Progress, Vol. 29, No. 335, pages 166-170, July.

[23] SWAN2 2002 (2002), User Manual: Ship Flow Simulation in Calm Water and in Waves, Boston Marine Consulting Inc., Boston MA 02116, USA.

[24] Sclavounos P.D. (1996), Computation of Wave Ship Interactions, Advances in Marine Hydrodynamics, ed. by M. Qhkusu, Computational Mechanics Publication.

[25] Kring D.C., Huang Y.F., Sclavounos P.D., Vada T., and Braathen A. (1996), Nonlinear ship motions and wave induced loads by a Rankine panel method, 21th Symposium of Naval Hydrodynamics, Trondheim, pp. 45-63.

[26] Yen T., Zhang S., Weems K., Lin W.M. (2010), Development and Validation of Numerical Simulations for Ship Maneuvering in Calm Water and in Waves, The Proceedings of the 28th Symposium of Naval Hydrodynamics , Pasadena, California, USA.

[27] Lin W.M., Zhang S., Weems K., and Yue D.K.P. (1999), A Mixed Source Formulation for Nonlinear Ship-Motion and Wave-Load Simulations, Proceedings of the 7th International Conference on Numerical Ship Hydrodynamics, Nantes, France, pp. 1.3.1–12.

[28] Lin W.M., Zhang S., Weems K., Liut D. (2006), Numerical Simulations of Ship Maneuvering in Waves, Proceedings of the 26th Symposium on Naval Hydrodynamics, Rome, Italy.

[29] Hooft J.P. (1994), The cross flow drag on a maneuvering ship, Ocean Engineering, 21(3):329-342.

[30] Toxopeus S.L. (2006), Validation of slender-body method for prediction of linear maneuvering coefficients using experiments and viscous-flow calculations, 7th ICHD International Conference on Hydrodynamics, pages 589-598, Ischia, Italy, October.

[31] Himeno Y. (1981), Prediction of Ship Roll Damping – State of the Art, University of Michigan, Report No. 239.